

Membranes with Fast and Selective Gas-Transport Channels of Laminar Graphene Oxide for Efficient CO₂ Capture**

Jie Shen, Gongping Liu, Kang Huang, Wanqin Jin,* Kueir-Rarn Lee, and Nanping Xu

Abstract: Graphene oxide (GO) nanosheets were engineered to be assembled into laminar structures having fast and selective transport channels for gas separation. With molecular-sieving interlayer spaces and straight diffusion pathways, the GO laminates endowed as-prepared membranes with excellent preferential CO₂ permeation performance (CO₂ permeability: 100 Barrer, CO₂/N₂ selectivity: 91) and extraordinary operational stability (> 6000 min), which are attractive for implementation of practical CO₂ capture.

Graphene is a well-known two-dimensional material that exhibits preminent electrical, mechanical, and thermal properties owing to its unique one-atom-thick structure.^[1] As an oxidized form of graphene, graphene oxide (GO) has a variety of oxygen-containing groups together with a laminar structure, showing great potential in membranes for molecular separation.^[2] The pioneering work of Geim et al.^[3] found that GO membranes are impermeable to gases and liquids but solely allow unimpeded evaporation of water. Thus, GO membranes have been reported for application in water-purification and solvent-dehydration processes.^[4] Meanwhile, recent works found that GO membranes can also exhibit gas-separation characteristics if their stacking structure is carefully controlled. Only two breakthroughs have been achieved to date. Kim et al.^[5] reported that selective gas (CO₂ or H₂) diffusion through few-layered GO membranes can be achieved by controlling gas-flow pathways and pores. Li et al.^[6] showed that structural defects on molecular-sieving GO membranes provided highly selective H₂ permeation over CO₂ and N₂. It seems that different fabrication approaches would lead to GO membranes with distinct microstructures and separation properties.

Until now, the preparation of GO membranes has been mostly based on using an aqueous environment. GO nano-

sheets are dispersed in water and then processed using filtration, dip coating, or spin coating; after evaporating the water, the GO membrane is finally formed. However, there are still many challenges these GO membranes have to confront. For example, free-standing GO membranes without substrates or brittle GO membranes with no reliable modules are difficult to use in practical applications.^[4e] Our previous work demonstrated a scalable fabrication of a GO membrane on a ceramic hollow fiber substrate, and the membrane showed highly selective molecular separation of an aqueous organic solution.^[7] Another problem is the assembly of GO into membranes by the application of external forces (e.g., pressure, centrifugal force) generally face the difficulty of precise and reproducible tuning of the membrane-processing parameters. The repulsive electrostatic interactions caused by negatively charged carboxy groups are prone to generate the inevitable non-selective defects in the GO membrane.^[5] Herein, we report a methodology for fabricating membranes that involves GO assembly in polymeric environment (Figure 1a). The key concept of this methodology is the construction and utilization of favorable molecular interactions between GO and the polymer to stimulate the stacking of GO nanosheets into well-defined GO laminates, in which the interlayer spaces could provide molecular-sieving channels.

GO nanosheets contain many hydroxy, carbonyl, and carboxy groups that are all highly polarized, with oxygen

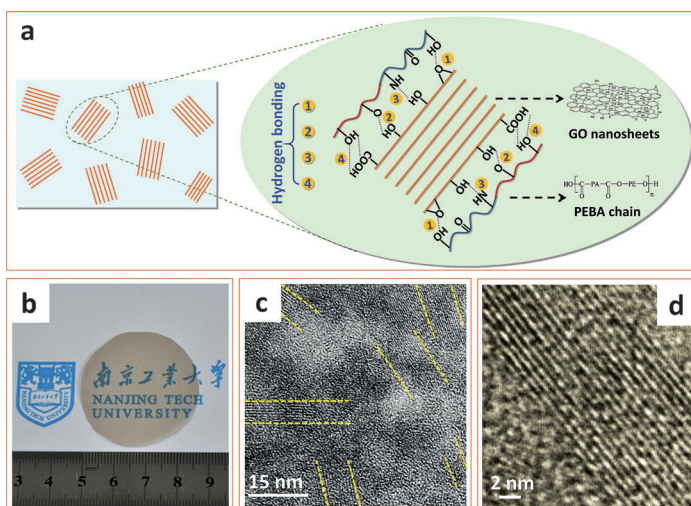


Figure 1. a) Schematic representation of the assembly of GO nanosheets in polymeric environment based on hydrogen bonds formed between different groups on GO and the PEBA chain, b) digital photographs of the membrane with 0.1 wt% GO, and c) overview (the yellow dashed lines are eye-guiding lines indicating the GO laminates in these regions) and d) expanded TEM image of the cross section of GO-1 membrane.

[*] J. Shen,^[†] Dr. G. Liu,^[†] K. Huang, Prof. W. Jin, Prof. N. Xu
State Key Laboratory of Materials-Oriented Chemical Engineering,
Nanjing Tech University (former Nanjing University of Technology)
5 Xinmofan Road, Nanjing 210009 (P.R. China)
E-mail: wqjin@njtech.edu.cn

Prof. K. Lee
R&D Center for Membrane Technology
Department of Chemical Engineering
Chung Yuan University, Chung-Li 32023 (Taiwan)

[†] These authors contributed equally to this work.

[**] This work was financially supported by the National Natural Science Foundation of China (Nos. 21476107, 21406107) and Innovative Research Team Program by the Ministry of Education of China (No. IRT13070).

Supporting information for this article is available on the WWW under <http://dx.doi.org/10.1002/ange.201409563>.

atoms being the negative center (Supporting Information (SI), FTIR spectra in Figure S1). This chemical characteristic is beneficial for the generation of hydrogen bonding, especially in the case of a high O/C ratio on GO (Supporting Information, XPS spectra in Figure S2).^[8] We thus selected polyether block amide (PEBA), a commercialized block copolymer containing -N-H-, H-N-C=O, and O-C=O groups, and an ethanol/water mixed solvent to disperse GO nanosheets in the polymeric matrix. Membranes with GO concentrations of 0.05, 0.075, and 0.1 wt% were fabricated and denoted as GO-05, GO-075, and GO-1, respectively. Numerous hydrogen bonds formed between different groups on GO and the PEBA chain, which are confirmed by FTIR and X-ray photoelectron spectroscopy (XPS) analysis (see Figure S3–S4 and detailed discussions in Supporting Information). Thus, in addition to the inherent hydrogen bonds between GO nanosheets,^[2] the hydrogen bonding caused by introducing polymer chains brings about a totally different assembly behavior and stacking structures of GO nanosheets in the membranes.

Figure 1b displays digital photographs of the as-prepared free-standing membrane with 0.1 wt% GO. It appears yellow and transparent, indicating uniform GO dispersion.^[2] AFM images show that the membrane surface was dispersed with homogeneous flake-like bulges, and their number increase with GO concentration, leading to a gradual increase of surface roughness (Figure S5). We consider that single-layered GO nanosheets would be assembled into few-layered laminates driven by the GO-PEBA hydrogen-bonding interactions (Figure S6). This was further confirmed by TEM observation of the membrane cross section, shown in Figure 1c. The laminar GO nanosheets are surrounded by the amorphous PEBA polymeric domains, and their thickness ranges from 6 to 15 nm. The regular laminar structures are clearly seen in the amplified image shown in Figure 1d, indicating that the *d*-spacing (*d*) of the GO laminate given by TEM is approximately 0.7 nm, which is smaller than that of the reported GO gas-separation membrane derived from an aqueous environment (*d* = 0.79 nm).^[6] This change is mainly attributed to the confinement effects of the polymeric chains and hydrogen bonding between GO and PEBA.^[9] The reduced size of the GO *d*-spacing would lead to enhanced molecular-sieving properties for gas separation. Considering that the *d*-spacing also includes the graphene thickness (0.35 nm),^[3] the interlayer spacing can be calculated to approximately 0.35 nm, which can be expected to be empty space for molecular transport.^[4a] The size of the space is in the range of the molecular kinetic diameters of industrial gases, such as CH₄ (0.38 nm), N₂ (0.36 nm), CO₂ (0.33 nm), and H₂ (0.29 nm). Thus, the membrane with GO laminates would provide selective transport channels for gas separation.

Usually, GO membranes are formed by the deposition of GO nanosheets into thin layers having inter-layer structures with different degrees of interlocking.^[10] The GO sheets were believed to be impermeable, and the small-molecule separation by GO membranes is based on the defect regions or boundaries of the GO sheets.^[4a,5,6] In contrast, this work demonstrates that an as-prepared membrane based on a polymeric environment enables the assembly of GO

nanosheets into GO stacks in random directions (Figure 1c). In addition to the tortuous pathways through parallel-stacked GO nanosheets,^[3] there are more straight and upright pathways provided by the inclined and even vertical GO stacks (Figure S7). As Geim and co-workers estimated,^[4a] the effective transport length of GO laminates with parallel stacks is $L \times h/d$, where *L* represents the length of the GO nanosheets, *h* the membrane thickness, and *d* the *d*-spacing. According to the AFM image of GO nanosheets (Figure S6) and TEM characterization of GO laminates (Figure 1d), we assumed *h* and *d* to be 500 nm and 0.7 nm, respectively. So the vertical GO stacks of our membrane have a very short transport distance (it equals *L*), which is 700 times shorter than that of the parallel stacks. It can be expected that these straight pathways of the GO laminates in the as-prepared membrane afford fast transport channels for gas molecules.^[11]

The fast and selective gas-transport channels of the GO laminates were studied by measuring the gas permeation properties through the as-prepared membranes. As shown in Figure 2a, the membranes allowed fastest transport for CO₂ molecules and very low permeation of other gases, with a gas permeability order of CO₂ > H₂ > CH₄ > N₂. Moreover, by increasing the number of GO nanosheets, both the CO₂ permeability and selectivity of the membrane are significantly enhanced, breaking the permeability/selectivity trade-off relation in polymeric membranes.^[12] The gas-transport behavior means that fast and selective CO₂ transport channels were provided by the regular laminar GO structures in these membranes. The CO₂ permeability reaches 100 Barrer and CO₂/N₂ selectivity is 91. As illustrated in Figure 2b, the separation performance of GO-1 for CO₂/N₂ transcends the upper bound for the reported polymeric membranes, including thermally rearranged (TR) polymers, polymers of intrinsic microporosity (PIM), and inorganic membranes, such as carbon, silica, and zeolite, as well as mixed-matrix membranes.^[5,13] The CO₂/H₂ separation performance also surpasses the permeability/selectivity map, as was reported by Freeman et al. in 2006 (Figure S8).^[14] Moreover, a continuous permeation of CO₂ and N₂ was carried out for 6000 min (Figure 2c). After this time no defects were found in the GO-1, indicating our membranes are very stable for practical application. To our knowledge, it is the first time such long-term stability has been realized with graphene-based membranes. The unprecedented preferential CO₂ permeation could be due to the unique characteristics of the GO laminates.

Generally, molecular permeation through gas-separation membranes is determined by two crucial properties: solubility and diffusivity.^[11] Strong specific affinity and molecular sieving effects, in addition to straight diffusion pathways, are beneficial for making highly permeable and selective membranes. The overall size distribution of cavities in the as-prepared membranes was analyzed by using the positron annihilation lifetime spectroscopy technique. In general, a longer *o*-positronium (*o*-Ps) lifetime suggests larger cavity sizes. As displayed in Figure 3a, the lifetime distribution is narrower in GO-1, accompanied by a reduction in the *o*-Ps lifetime, τ_3 , and an improvement of the *o*-Ps intensity, *I*₃, which indicate enhanced molecular sieving ability and cavity

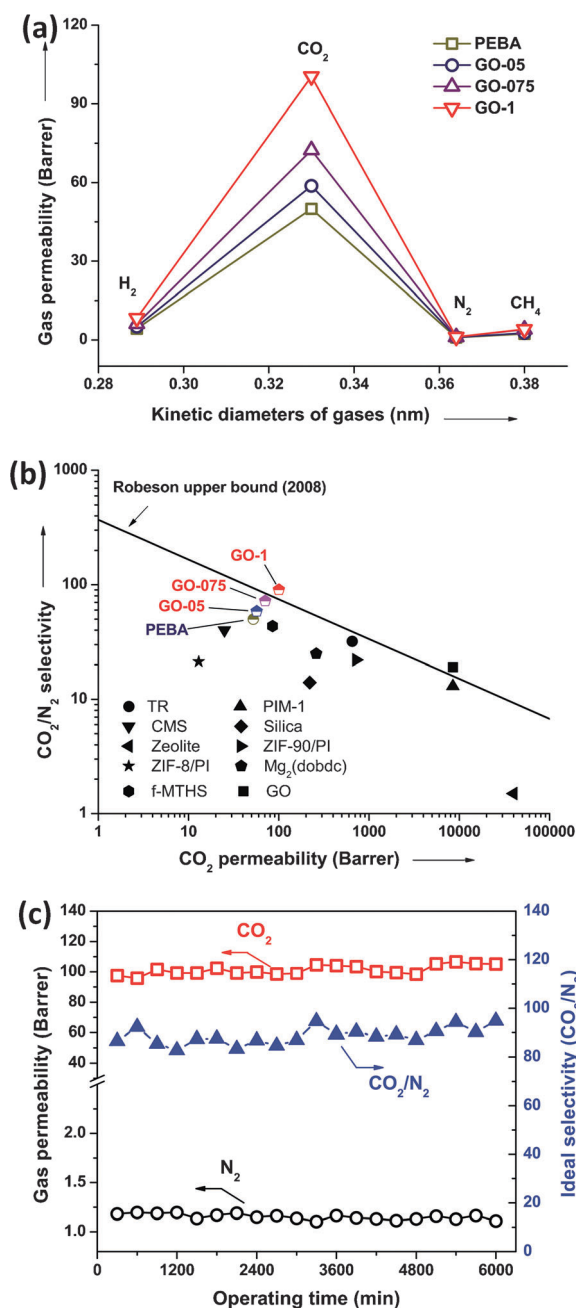


Figure 2. Gas permeation through the membranes with different GO concentrations: a) permeabilities of H₂, CO₂, N₂, and CH₄; b) CO₂/N₂ separation performance of PEBA, GO-05, GO-075, and GO-1 membranes and representative membranes reported in the literature, and c) long-term operation test of CO₂/N₂ for GO-1 membrane. The gas permeation tests were measured at 0.3 MPa and 25 °C, 1 Bar-rer = 10⁻¹⁰ cm³ (STP) cm/(cm² s cmHg).

numbers for diffusion. The cavity numbers and/or cavity size of the bare PEBA membrane are thought to decrease after incorporation of GO-1 owing to the abundant hydrogen bonds between GO and PEBA. This can be inferred from the gradual improvement of the glass transition temperature of PEBA with increasing GO amount (Figure S9). Thus, the GO laminates are considered to create a large number of cavities that are expected to be more numerous than the ones

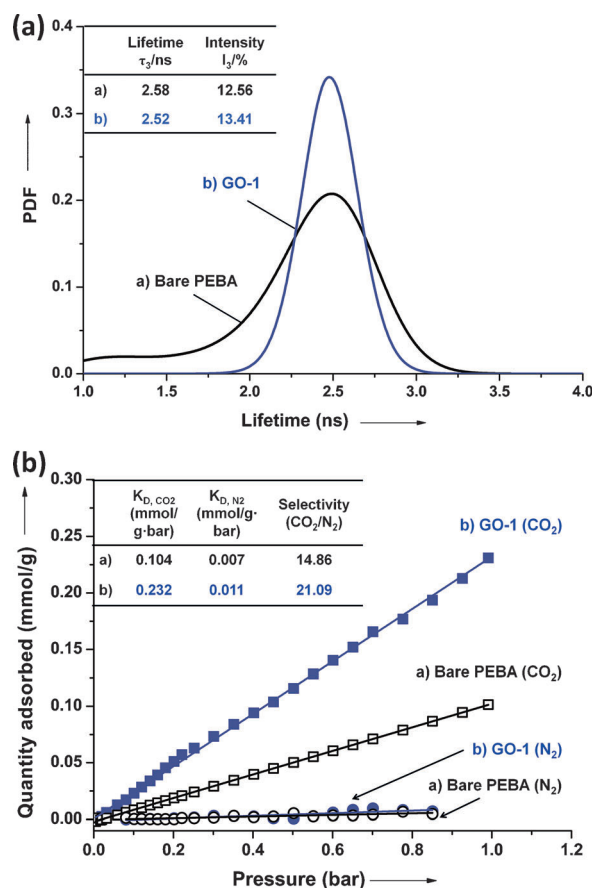


Figure 3. a) Positron annihilation lifetime spectra of bare PEBA and GO-1 membranes and b) pure-component CO₂ and N₂ adsorptions on PEBA and GO-1 membrane, both of which employ single-site Langmuir models, K_D is Henry's constant.

corresponding to the increased *o*-Ps intensity (Table inset in Figure 3a). Moreover, TEM observation shows that the interlayer spacing of the GO laminates is approximately 0.35 nm, which allows a cutoff in permeation for molecules with kinetic diameters greater than this value. The channels exhibit a molecule-sieving effect and thus gas could diffuse selectively through the membrane. As shown in Figure 2a, with the increase of GO amount, the permeabilities of CO₂ and H₂ are progressively enhanced, whereas those of N₂ and CH₄ show little change, leading to the significantly improvement of selectivities for CO₂/N₂ and CO₂/CH₄ pairs (Figure S10).

In addition, the specific adsorption of CO₂ in the GO laminates further accelerates the preferential CO₂ transport through the membrane. Li et al. found that the gas adsorption of GO powders followed the order of CO₂ > CH₄ > N₂ > H₂.^[6] We measured the gas adsorption behaviors on GO-1 and a typical result of CO₂/N₂ adsorption is shown in Figure 3b. Because of the favorable interactions between the polar groups such as -COOH, -OH on GO, and the polar individual C-O bonds on CO₂,^[5] the GO laminates in the membrane contribute to 2.2 times higher CO₂ adsorption than that could be obtained with the bare PEBA membrane. Meanwhile, the CO₂/N₂ adsorption selectivity also increased by 42% (Table

inset in Figure 3b). Although H_2 molecules are supposed to diffuse much faster than CO_2 according to their smaller kinetic diameter, the permeability of CO_2 is 12 times higher than that of H_2 (Figure 2a). This is owing to the high adsorption selectivity of CO_2/H_2 resulting from the GO laminates. Therefore, we speculated that by exhibiting preferential CO_2 adsorption and diffusion, the laminar GO nanosheets in the as-prepared membrane create fast and selective transport channels for CO_2 molecules.

To further verify our inference, we reduced the GO-1 membrane by heating it at $150^\circ C$, based on thermogravimetric analysis (TGA) of the GO powder and PEBA (Figure S11), and we measured the permeability variations of CO_2 , H_2 , and N_2 . The reduction process is considered to have two effects on molecular transport: 1) narrowing the interlayer spacing in the GO laminates,^[6] thus limiting the permeation of CO_2 and H_2 through the channels, and 2) decreasing the number of oxygen-containing groups in the GO nanosheets,^[2] so as to weaken the CO_2 adsorption on the channels. It is interesting to find that the two non-specific adsorptive molecules, H_2 and N_2 , exhibited disparate transport behaviors. As shown in Figure S12, H_2 permeation significantly decreased, whereas N_2 permeation was not affected by the GO reduction. The size-dependent permeation phenomenon confirms that the interlayer spacing of the GO laminates provided molecular-sieving channels for gas transport. Moreover, the fact that the permeability of CO_2 decreases much more than that of H_2 indicates that the synergy between specific adsorption and selective diffusion controlled the CO_2 transport through the GO channels.

As a very important prerequisite for the fast molecular transport, the uniform dispersion of GO stacks in the membrane needs to be realized. When GO stacks aggregate with each other, the diffusion of gas molecules through one GO stack would be hindered by other GO stacks oriented in different directions. We validated this speculation by fabricating membranes with high GO concentrations (0.2–0.5 wt %). GO aggregation was confirmed by AFM, TEM, digital photographs, and gas permeation tests (Figure S13–16). It was revealed that CO_2 and H_2 that could enter the GO channels showed significantly suppressed permeation with increasing GO concentration. However, there was little change in N_2 permeability because its larger molecular size leads it to diffuse around the GO laminates, and thus its transport is less affected by the GO aggregation. These characterizations also provide evidence of the key role of GO laminates with molecular-sieving interlayer spacing and straight diffusion pathways in determining the gas transport.

The fabrication feasibility and structural stability are two significant criteria required for GO-based membranes for practical applications.^[11] Thus the GO polymeric dispersion was tested and shown to be a superior approach in that membranes are able to be easily coated on various substrates of different configurations and materials, resulting in outstanding processability. We demonstrated the preparation of two popular industrial composite membranes with polymeric flat and inorganic hollow fiber substrates, respectively.^[15] FESEM images of the membrane cross sections (Figure S17) show that uniform active layers are firmly adhered on the

porous substrates, with an average thickness of approximately $5\ \mu m$. The separation performance of the hollow fiber membrane with the GO concentration of 0.1 wt % (Figure S18) is comparable to that of the flat one (GO-1). Moreover, the hollow fiber composite membrane is robust, exhibiting excellent interfacial adhesion which is significant for long-term continuous operation. Its critical load at the interface determined by nanoindentation reaches 37.65 mN (Figure S19), indicating that there is a strong binding force between the active layer and substrate. Thus, our as-prepared membranes can be readily engineered to scale up, which is promising for industrialized implementation.

In conclusion, membranes with fast and selective CO_2 transport channels of GO laminates were proposed based on the construction of hydrogen bonding between GO and polymer, that enabled the assembly of GO nanosheets into several-layered GO stacks with molecular-sieving interlayer spacing and straight diffusion pathways. The as-prepared membrane featured excellent preferential CO_2 permeation characteristics, with an extraordinary high and stable CO_2/N_2 separation performance transcending the upper bounds of state-of-the-art membranes. With careful control of the polymer environment, the performance could be further improved by increasing the number of gas-transport channels of uniformly dispersed GO stacks in the membrane. Having distinct advantages in terms of facile fabrication and structural stability, the GO-based membrane reported herein offers great potential for practical CO_2 capture processes.

Received: September 29, 2014

Published online: November 5, 2014

Keywords: CO_2 capture · gas channels · graphene · graphene oxide · membranes

- [1] a) A. K. Geim, *Science* **2009**, 324, 1530–1534; b) C. N. R. Rao, A. K. Sood, K. S. Subrahmanyam, A. Govindaraj, *Angew. Chem. Int. Ed.* **2009**, 48, 7752–7777; *Angew. Chem.* **2009**, 121, 7890–7916.
- [2] D. R. Dreyer, S. Park, C. W. Bielawski, R. S. Ruoff, *Chem. Soc. Rev.* **2010**, 39, 228–240.
- [3] R. R. Nair, H. A. Wu, P. N. Jayaram, I. V. Grigorieva, A. K. Geim, *Science* **2012**, 335, 442–444.
- [4] a) R. K. Joshi, P. Carbone, F. C. Wang, V. G. Kravets, Y. Su, I. V. Grigorieva, H. A. Wu, A. K. Geim, R. R. Nair, *Science* **2014**, 343, 752–754; b) Y. Han, Z. Xu, C. Gao, *Adv. Funct. Mater.* **2013**, 23, 3693–3700; c) Y. P. Tang, D. R. Paul, T. S. Chung, *J. Membr. Sci.* **2014**, 458, 199–208; d) W.-S. Hung, C.-H. Tsou, M. De Guzman, Q.-F. An, Y.-L. Liu, Y.-M. Zhang, C.-C. Hu, K.-R. Lee, J.-Y. Lai, *Chem. Mater.* **2014**, 26, 2983–2990; e) B. Mi, *Science* **2014**, 343, 740–742; f) M. Hu, B. Mi, *Environ. Sci. Technol.* **2013**, 47, 3715–3723; g) Y. Lou, G. Liu, S. Liu, J. Shen, W. Jin, *Appl. Surf. Sci.* **2014**, 307, 631–637.
- [5] H. W. Kim, H. W. Yoon, S.-M. Yoon, B. M. Yoo, B. K. Ahn, Y. H. Cho, H. J. Shin, H. Yang, U. Paik, S. Kwon, J.-Y. Choi, H. B. Park, *Science* **2013**, 342, 91–95.
- [6] H. Li, Z. Song, X. Zhang, Y. Huang, S. Li, Y. Mao, H. J. Ploehn, Y. Bao, M. Yu, *Science* **2013**, 342, 95–98.
- [7] K. Huang, G. Liu, Y. Lou, Z. Dong, J. Shen, W. Jin, *Angew. Chem. Int. Ed.* **2014**, 53, 6929–6932; *Angew. Chem.* **2014**, 126, 7049–7052.

- [8] S. Stankovich, D. A. Dikin, G. H. B. Dommett, K. M. Kohlhaas, E. J. Zimney, E. A. Stach, R. D. Piner, S. T. Nguyen, R. S. Ruoff, *Nature* **2006**, *442*, 282–286.
- [9] H. Y. Jeong, J. Y. Kim, J. W. Kim, J. O. Hwang, J.-E. Kim, J. Y. Lee, T. H. Yoon, B. J. Cho, S. O. Kim, R. S. Ruoff, S.-Y. Choi, *Nano Lett.* **2010**, *10*, 4381–4386.
- [10] Z. P. Smith, B. D. Freeman, *Angew. Chem. Int. Ed.* **2014**, *53*, 10286–10288; *Angew. Chem.* **2014**, *126*, 10452–10454.
- [11] D. L. Gin, R. D. Noble, *Science* **2011**, *332*, 674–676.
- [12] a) B. D. Freeman, *Macromolecules* **1999**, *32*, 375–380; b) L. M. Robeson, *J. Membr. Sci.* **2008**, *320*, 390–400.
- [13] a) H. B. Park, C. H. Jung, Y. M. Lee, A. J. Hill, S. J. Pas, S. T. Mudie, E. Van Wagner, B. D. Freeman, D. J. Cookson, *Science* **2007**, *318*, 254–258; b) N. Du, H. B. Park, G. P. Robertson, M. M. Dal-Cin, T. Visser, L. Scoles, M. D. Guiver, *Nat. Mater.* **2011**, *10*, 372–375; c) T.-H. Bae, J. S. Lee, W. Qiu, W. J. Koros, C. W. Jones, S. Nair, *Angew. Chem. Int. Ed.* **2010**, *49*, 9863–9866; *Angew. Chem.* **2010**, *122*, 10059–10062; d) Q. Song, S. K. Nataraj, M. V. Roussanova, J. C. Tan, D. J. Hughes, W. Li, P. Bourgoïn, M. A. Alam, A. K. Cheetham, S. A. Al-Muhtaseb, E. Sivaniah, *Energy Environ. Sci.* **2012**, *5*, 8359–8369; e) T.-H. Bae, J. R. Long, *Energy Environ. Sci.* **2013**, *6*, 3565–3569; f) D. K. Roh, S. J. Kim, W. S. Chi, J. K. Kim, J. H. Kim, *Chem. Commun.* **2014**, *50*, 5717–5720.
- [14] H. Lin, E. Van Wagner, B. D. Freeman, L. G. Toy, R. P. Gupta, *Science* **2006**, *311*, 639–664.
- [15] A. J. Brown, N. A. Brunelli, K. Eum, F. Rashidi, J. R. Johnson, W. J. Koros, C. W. Jones, S. Nair, *Science* **2014**, *345*, 72–75.